crystals

MDPI

Porosity Distribution and Impure Inclusion Analysis of Porous Crystal Layer Formed via Polythermal Process

Yingshuang Meng, Zhonghua Li, Xiangcun Li, Wu Xiao, Gaohong He, Xuemei Wu and Xiaobin Jiang*

Research and Development Center of Membrane Science and Technology, State Key Laboratory of Fine Chemicals, School of Chemical Engineering, Dalian University of Technology, Dalian, Liaoning 116024, China

1. Gravity settling velocity u

Reynolds Number is defined as $\mathrm{Re_p} = d_s \rho u / \mu$; d_s is the equivalent diameter of the crystal. If $\mathrm{Re_p} \le 1$, laminar region, the gravity settling velocity u follows Stocks equation,

$$u = \frac{d_S^2(\rho_S - \rho)g}{18\mu} \quad (1)$$

if $1 < \mathrm{Re_p} \le 1000$, intermediate region, u follows Allen equation,

$$u = 0.27\sqrt{\frac{g d_s(\rho_s - \rho)\mathrm{Re}^{0.6}}{\rho}} \quad (2)$$

if $1000 < \mathrm{Re_p} \le 2\times10^5$, turbulent region, u follows Newton equation,

$$u_t = 1.74\sqrt{\frac{d(\rho_s - \rho)g}{\rho}} \quad (3)$$

2. The crystallization relevant data of the investigated systems

The physical and chemical data of the investigated crystallization system in this paper are listed in Table S1 (some of the data were measured in this work and some were cited from the reported literatures).

Table S1. Crystallization relevant data of the investigated systems in this paper.

System	m	k_g	ΔE_g, kJ mol^{-1}	a	ρ_S, kg m^{-3}	$\overline{\rho_S}/\rho_L$ *	$\overline{\mu}$ **, mPa s	Average aspect ratio of crystal	Date resource
Urea-H_2O	1.56	9.787×10-12	8.730	1.05	1.227	1.15	1.55	8	Measured in this article

* $\overline{\rho_{\mathrm{fluid}}}$ is the average density of the saturated fluid in the investigated situation.

** $\overline{\mu}$ is the average viscosity of the saturated fluid in the investigated situation.

Table S2. Solubility of Urea in Water.

Temp (℃)	0	10	20	30	40	50	60	70	ref
C_e (Moles/L)	6.6860	5.246	5.536	9.566	6.392	11.19	24.22	27.30	[1]

Table S3. Solubility of KNO_3 in Water.

Temp (℃)	0	10	20	30	40	50	60	70	ref
C_e (Moles/L)	1.1869	1.7408	2.3936	3.0959	3.8179	4.5201	5.1631	5.7367	[2]

1. Yalkowsky, Samuel, Yan, and Parijat Jain. *Handbook of Aqueous Solubility Data*. 2nd ed.; CRC Press, 2016; pp. 9–11.
2. Haynes, W. M. Thermochemistry, Electrochemistry, and Solution Chemistry. In *Handbook of Chemistry and Physics*. 95th ed.; Haynes, W. M.; CRC Press, 2014;pp.180–190.

3. Images of porosity distribution (PD) experiments

Schematic images of PD obtained in the experiments were shown as followed. The crystal layer was detected along the axial direction by MRI system. The images were arranged from left to right, then from top to the bottom, of the detecting order (the distance between two adjacent images was around 10 to 15 mm). The images indicated that determine the porosity by the image analysis may lead to predictable deviation. Thus, the mean relaxation time of T2 spectrum (obtained from the software in the MRI system) was introduced as the characteristic value of the porosity and normalized by the mean relaxation time of the top porous slice T2,0, which had been reported in many literatures.

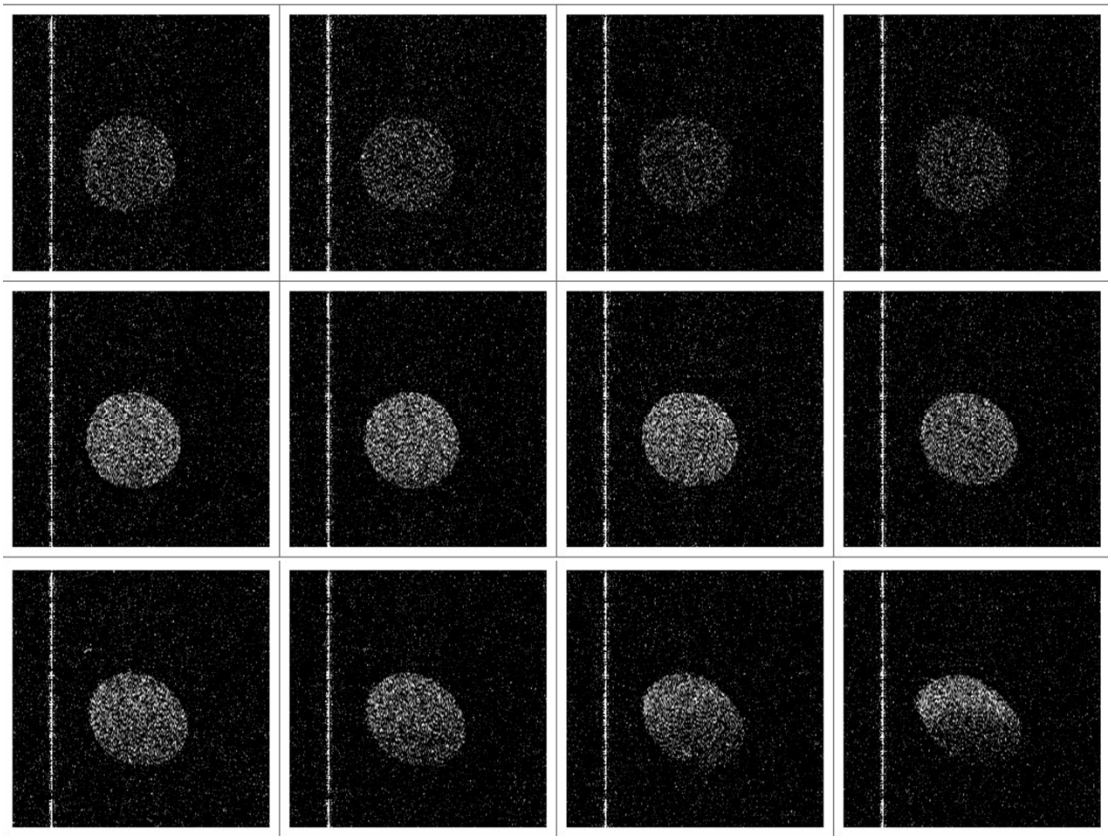

Figure S1. Images of PD obtained by MRI system experiments (1).

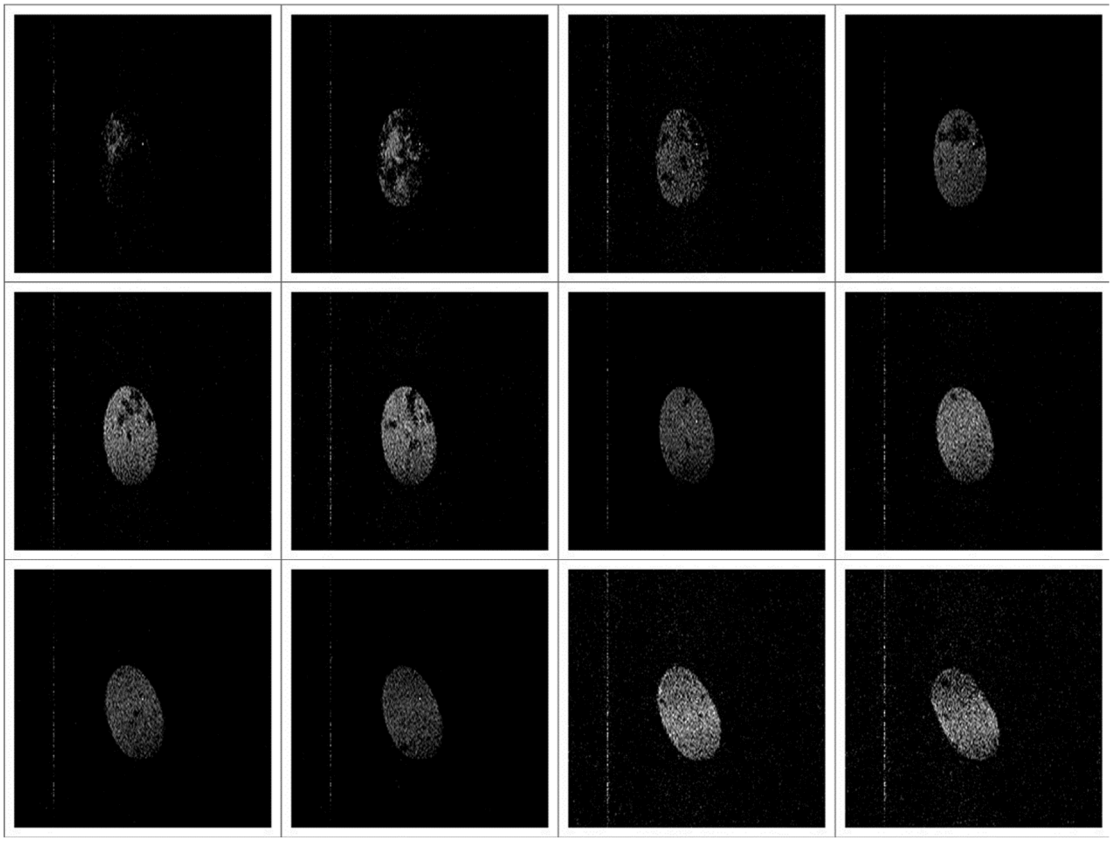

Figure S2. Images of PD obtained by MRI system experiments (2).

4. The morphology research of the porous crystal slice, the fractal nucleation and growth.

A flat crystallizer (inner diameter 40 mm, height 25 mm, self-made) with a jacket around its wall (no jacket on the bottom side) was implemented to simulate the formation of the single crystal slice. A crystallization solution with a known concentration was added and kept at the saturating temperature by a microcomputer-controlled thermostatic bath with the precision of ±0.1 K (CKDC, Nanjing FDL Co., Ltd., China). A predetermined temperature profile was used in the experiments to acquire the degree of supercooling demanded. The experimental setup was shown in Fig. S3.

The images of the crystal nucleation and growth were automatically captured by an inverted fluorescence microscope (AE31, amplification: 40x to 600x, Motic China Group Co., Ltd., China) coupled with a digital imaging system (Motic 252B, image resolution: 2080*1542 effective pixels, Motic China Group Co., Ltd., China). The images were analyzed by Images Advanced 3.2 assisted by Motic 252B.

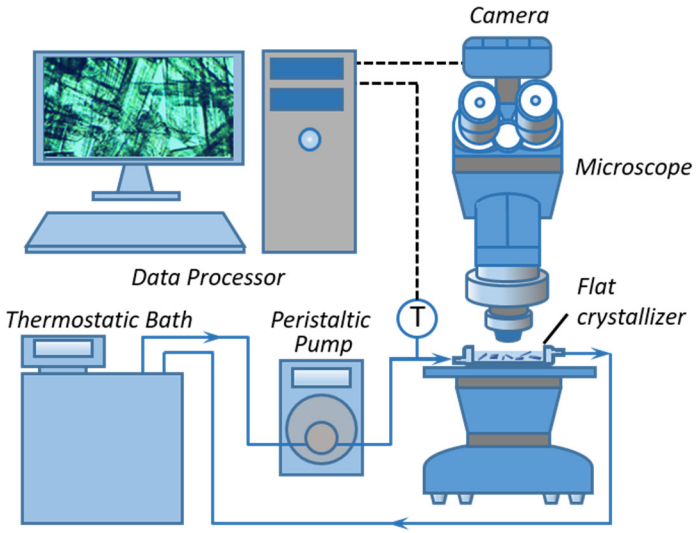

Figure S3. Experimental apparatus for the imitative porous crystal slice.

The images obtained by the inverted fluorescence microscope coupled with a digital imaging system during formation of the porous crystal slice are shown in Fig. S4 (urea aqueous solution, T_e= 308 K, initial degree of supercooling = 2 K, cooling rate v = 1.0 K·min^{-1}). The crystal nucleus and the initial crystal particles can be observed with high magnification optics (Fig. S4B). The stochastic crystal nuclear distribution and establishment of the crystal framework were also detected in Fig. S4C and S4D. In addition, the desired crystal growth frontier can be seen when there is an abundant gap left to be occupied (Fig. S4E). With the crystal growth, the gap filled by the supercooled solution is gradually occupied by the crystal framework. The gap left for the fluid transport becomes tortuous, and then, the porous crystal slice is eventually formed (Fig. S4F). Considering the fast crystal growth on the preponderant growth interface under a high degree of supercooling, the length of the crystal particles varied with the different supercooling conditions and the size of the crystallizer utilized.

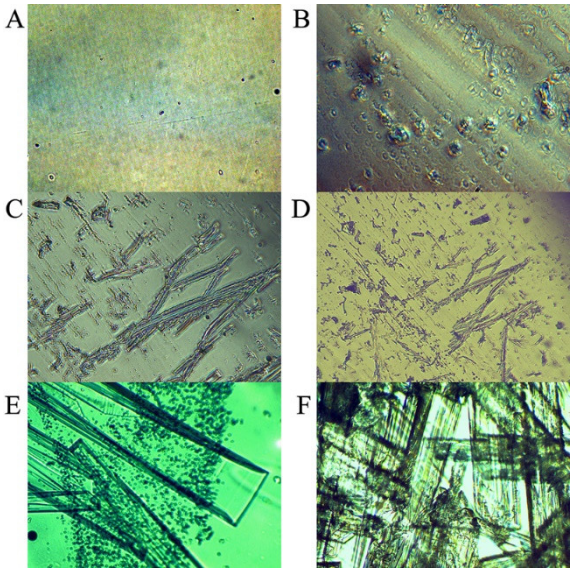

Figure S4. The images of the formation procedure for the porous crystal slice. (A)×600, t = 0 s; (B) ×400, t = 10 s; (C) ×100, t = 30 s; (D) ×40, t = 30 s; (E) ×100, t = 120 s; (F) ×40, t = 330 s.

Compared to the rapid nucleation and growth process under the exceedingly high degree of supercooling and cooling rate, the gradient freezing process (also a polythermal process) within the metastable zone of the crystallization system was carried out to investigate the spatial distribution of the initial nucleus (Fig. S5). Under the metastable state polythermal process, nucleation clearly tended to occur preferentially at the heterogeneous interface. Moreover, the nucleus spatial distribution and size approximately followed self-similarity, which indicated that the porous channel established in the following porous crystal layer growth possessed the possible fractal properties. The multiscale branched structure was established under stepwise growth. The complex porous crystal layer was then formed in this structure. The detailed description of this detected fractal structure will be meaningful for an in-depth understanding of the stochastic crystal nucleus and porous structure formation.

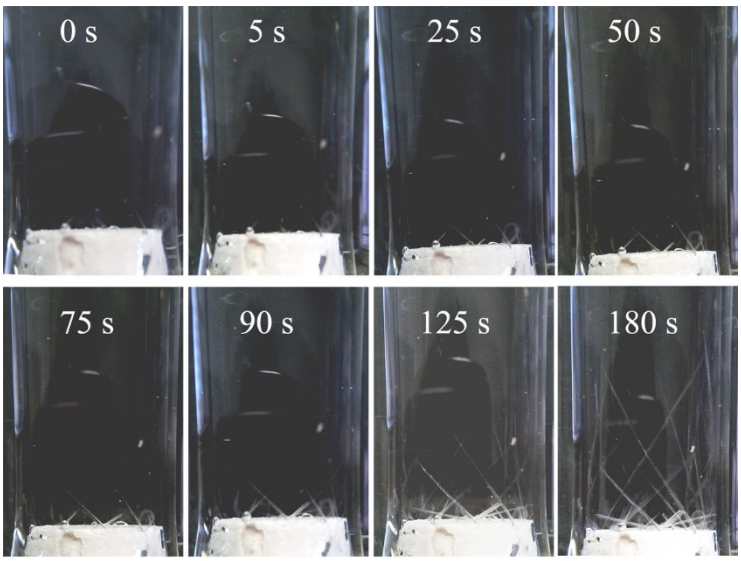

Figure S5. The detailed image of the initial nucleus distribution and growth at the bottom of the crystal tower. (urea aqueous solution, T_e = 308 K, initial degree of supercooling = 2 K, cooling rate v = 0.5 K·min^{-1}).